JES
JOURNAL OF ENVIRONMENTAL SCIENCES
ISSN 1001-0742
CN 11-2629/X
September 1, 2014 Volume 26 Number 9
www.jesc.ac.cn

Management of P in Agricultural Systems

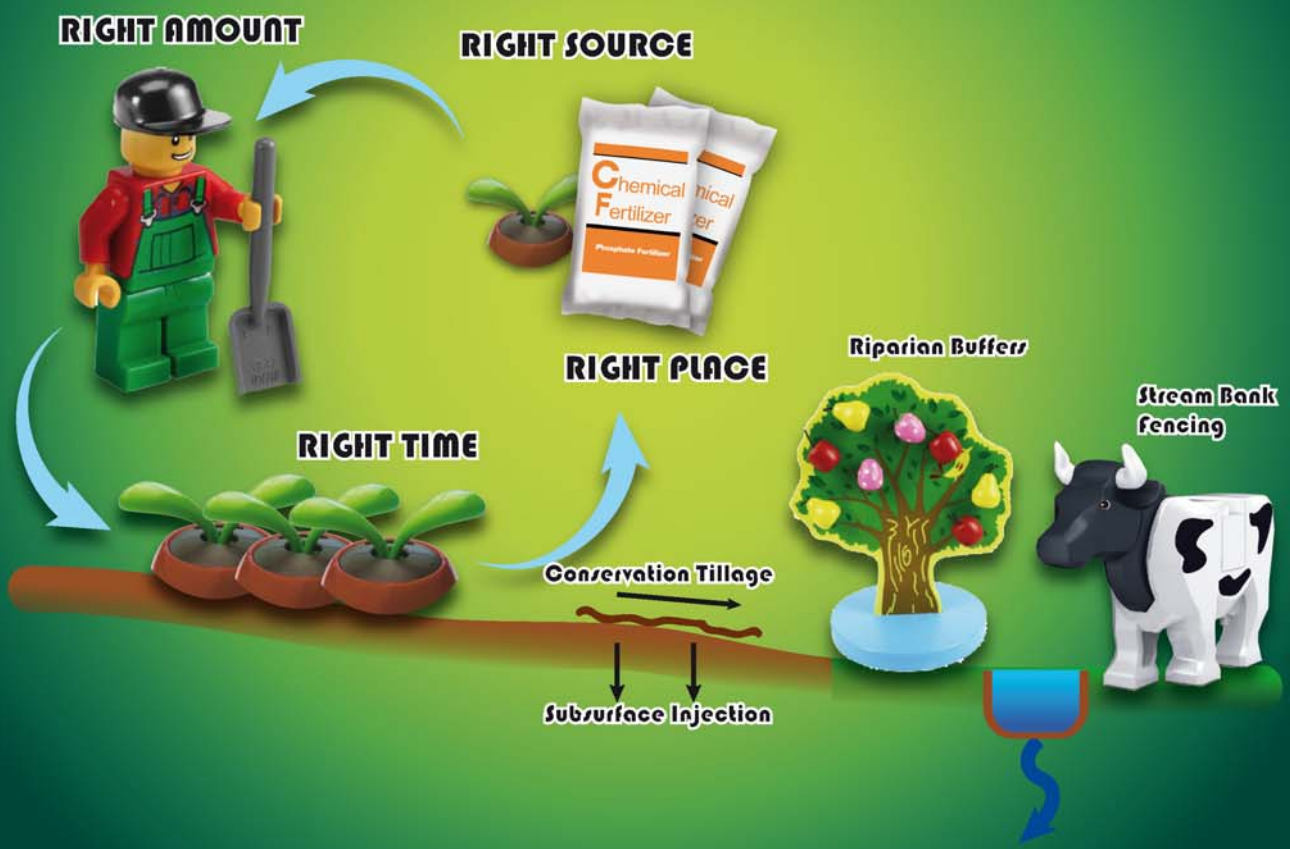

ELSEVIER
Science Press
Sponsored by
Research Center for Eco-Environmental Sciences
Chinese Academy of Sciences

Journal of Environmental Sciences Volume 26 Number 9 2014

www.jesc.ac.cn

CONTENTS

JOURNAL OF ENVIRONMENTAL SCIENCES 26 (2014) 1936–1942

Available online at www.sciencedirect.com

ScienceDirect

www.journals.elsevier.com/journal-of-environmental-sciences

Synthesis of novel CeO_2–$BiVO_4$/FAC composites with enhanced visible-light photocatalytic properties

Jin Zhang[1,2], *Bing Wang*[1], *Chuang Li*[1], *Hao Cui*[1], *Jianping Zhai*[1], *Qin Li*[1,*]

1. *State Key Laboratory of Pollution Control and Resource Reuse, School of the Environment, Nanjing University, Nanjing 210023, China. E-mail: jzmary@163.com*

2. *School of Biochemical and Environmental Engineering, Nanjing Xiaozhuang University, Nanjing 211171, China*

ARTICLE INFO

Article history:
Received 25 October 2013
Revised 1 December 2013
Accepted 28 January 2014
Available online 16 July 2014

Keywords:
CeO_2
$BiVO_4$
Fly ash cenospheres (FACs)
Photocatalysis
Composites

ABSTRACT

To utilize visible light more effectively in photocatalytic reactions, a fly ash cenosphere (FAC)-supported CeO_2–$BiVO_4$ (CeO_2–$BiVO_4$/FAC) composite photocatalyst was prepared by modified metalorganic decomposition and impregnation methods. The physical and photophysical properties of the composite have been characterized by X-ray diffraction (XRD), scanning electron microscope (SEM) and energy dispersive X-ray spectroscopy (EDX), X-ray photoelectron spectroscopy (XPS), and UV–Visible diffuse reflectance spectra. The XRD patterns exhibited characteristic diffraction peaks of both $BiVO_4$ and CeO_2 crystalline phases. The XPS results showed that Ce was present as both Ce^{4+} and Ce^{3+} oxidation states in CeO_2 and dispersed on the surface of $BiVO_4$ to constitute a p–n heterojunction composite. The absorption threshold of the CeO_2–$BiVO_4$/FAC composite shifted to a longer wavelength in the UV–Vis absorption spectrum compared to the pure CeO_2 and pure $BiVO_4$. The composites exhibited enhanced photocatalytic activity for Methylene Blue (MB) degradation under visible light irradiation. It was found that the 7.5 wt.% CeO_2–$BiVO_4$/FAC composite showed the highest photocatalytic activity for MB dye wastewater treatment.

© 2014 The Research Center for Eco-Environmental Sciences, Chinese Academy of Sciences. Published by Elsevier B.V.

Introduction

Visible-light-driven photocatalysis as a green energy technology has attracted a great deal of research interest due to its potential applications in water splitting and environmental remediation (Jeong et al., 2013; Wang et al., 2012). Therefore the development of photocatalysts responsive to visible light has attracted much attention in recent years. Among the photocatalysts recently reported, $BiVO_4$, with a monoclinic scheelite structure, shows good photocatalytic performance under visible light irradiation (Obregón et al., 2012; Naya et al., 2011). Monoclinic $BiVO_4$ has a band gap energy of 2.4 eV and can absorb the solar spectrum fraction up to blue light of ca. 520 nm, which is much more effective than that of TiO_2 photocatalyst (3.2 eV) for utilization of solar energy. However, the photocatalytic activity of pure $BiVO_4$ is unsatisfactory for practical applications, due to its poor absorption performance and difficult migration of photo-generated electron–hole pairs under visible light irradiation (Zhao et al., 2012).

Many attempts have been made to improve the photocatalytic activity of $BiVO_4$ in visible light irradiation, such as phase/morphological control, doping, noble metal loading, and design of composite materials (Ren et al., 2009; Won et al., 2012; Park et al., 2011; Zhao et al., 2013). Composite semiconductors have been reported to have potential as photocatalysts because they can reduce the recombination of photogenerated electron–hole pairs, and therefore can enhance the quantum yield (Ma et al., 2012). Zhou et al. (2012) found that an Ag–AgCl/$BiVO_4$ composite powder exhibited significantly enhanced photocatalytic activity in dye degradation. Jang et al. (2012) synthesized MO (CuO, Co_3O_4 and NiO)/$BiVO_4$ junction composites, and found that the photocatalysts could achieve efficient charge

* *Corresponding author*. E-mail: qli@nju.edu.cn (Qin Li).

http://dx.doi.org/10.1016/j.jes.2014.07.006
1001-0742/© 2014 The Research Center for Eco-Environmental Sciences, Chinese Academy of Sciences. Published by Elsevier B.V.

separation and showed enhanced photocatalytic activity in Acid Orange dye decomposition. Fu et al. (2011) reported that $BiVO_4$/graphene composites showed superior photoactivity in the degradation of dyes under visible light irradiation, and the significant enhancement in photoactivity can be ascribed to the concerted effects of $BiVO_4$ and graphene sheets or their integrated properties.

In our present study, $BiVO_4$ was coupled with CeO_2 with the expectation of obtaining a promising visible-light driven catalyst. CeO_2 itself has some properties like the commonly used photocatalyst TiO_2, such as wide band gap, nontoxicity, high stability, strong absorption in the UV region, and good photocatalytic activity under UV irradiation (Shao and Ma, 2012; Hernández-Alonso et al., 2004). In addition, CeO_2 is a p-type semiconductor with the potential to create sufficient conduction/valence band positions to promote charge separation when in contact with an *n*-type semiconductor (Kubacka et al., 2012). Such a possibility has been exploited to obtain visible-active composite photocatalysts (Muńoz-Batista et al., 2013; Foletto et al., 2012). Wetchakun et al. (2012) sought to narrow the band gap energy of CeO_2 photocatalysts by forming heterojunctions between CeO_2 and $BiVO_4$ in order to generate visible light-driven catalysts, and the as-prepared $BiVO_4/CeO_2$ nanocomposite exhibited excellent photocatalytic activity in dye wastewater treatment.

However, both $BiVO_4$-based composites and $BiVO_4/CeO_2$ nanocomposites have the same problems, including their fixation, diffusion and recycling. Coating the particles onto a support is a promising method to resolve this problem. In addition, supported catalysis has been awarded the status of "green" chemistry because it allows easy separation of the products and permits the recycling and reuse of the catalysts, giving both operational and economical advantages (Zhang et al., 2009). Herein, we attempt to support a CeO_2–$BiVO_4$ composite over fly ash cenospheres (FACs), an aluminosilicate-rich by-product of coal-fired power plants. FACs have been used as substrates in many studies due to their advantageous properties, such as low cost, chemical/physical stability, low density and nontoxicity (Pang et al., 2012). In this article, the composite, using FACs as the support for the CeO_2–$BiVO_4$ hybrid oxide, was synthesized by a combination of modified metalorganic decomposition (MOD) and impregnation methods. The physical and photophysical properties of the composite were characterized, and its photocatalytic ability was evaluated using the degradation of Methylene Blue (MB) in aqueous solution under visible light irradiation. The as-prepared CeO_2–$BiVO_4$/FAC composites showed interesting photocatalytic activity, suggesting that this CeO_2–$BiVO_4$/FAC system could be a promising environmental catalyst system.

1. Materials and methods

1.1. Raw materials and reagents

FACs were obtained from Nanjing Jinling Petrochemical Company. Then the FACs were sieved and the particles with the size range of 100–125 μm were chosen as the subsequent experimental material. The pretreatment and surface modification of FACs were discussed in a previous paper (Zhang et al., 2013). All other chemicals were of analytical grade and used without further purification.

1.2. Preparation of CeO_2–$BiVO_4$/FAC composites

The $BiVO_4$ films coated on FACs were prepared by the MOD method (Galembeck and Alves, 2002). In a typical process, 7.27 g $Bi(NO_3)_3{\cdot}5H_2O$ was dissolved in 75 mL acetic acid and 3.6 mL vanadium (V) tri-i-propoxy oxide was dissolved in 75 mL acetylacetone. The two resulting solutions were mixed to form a dark-green sol, which was then stirred vigorously for 1 hr before 10.2 g FAC was added, and the mixture was stirred for a further 3 hr at room temperature. The mixture thus obtained was evaporated at 85°C in a water bath, dried at 110°C for 6 hr, and then annealed in air at 500°C for 2 hr. The as-prepared samples are hereafter denoted $BiVO_4$/FACs.

The CeO_2–$BiVO_4$/FAC catalysts were prepared using an impregnation method. $BiVO_4$/FACs and an appropriate amount of aqueous $Ce(NO_3)_3{\cdot}6H_2O$ solution were mixed in a ceramic dish and the suspension was evaporated over a water bath at 85°C followed by calcination in air at 400°C for 4 hr to obtain composites. The composites were denoted as *x* wt.% CeO_2–$BiVO_4$/FACs (*x* = 2.5, 5, 7.5, 10).

1.3. Characterization

The crystal phases of the prepared composites were identified using an X-ray diffractometer (XRD, X′-TRA, ARL, Switzerland) with Cu Kα radiation (λ = 0.15418 nm). The surface morphology and composition were observed with a scanning electron spectroscope (S-3400NII, Hitachi, Japan) and energy dispersive X-ray spectroscopy (EDX, EX-250, Horiba, Japan) attached to this scanning electron microscope (SEM), respectively. The surface electronic states were determined by X-ray photoelectron spectroscopy (XPS, PHI5000, ULVAC-PHI, Japan) with an Al Kα X-ray source (1486.6 eV). The optical properties were analyzed by UV–vis diffuse reflectance spectroscopy (UV-2450, Shimadzu, Japan).

1.4. Photocatalytic degradation of MB

The photocatalytic activity of the CeO_2–$BiVO_4$/FAC composite was evaluated by the degradation of MB under visible light irradiation using an XPA photochemical reactor (XPA-2, Xujiang Factory of Electrical Engineering, China). The reaction vessel was thermostated at 25°C with a water cooling jacket. A 500 W Xe lamp was used as the light source with a cut-off filter to remove all wavelengths lower than 420 nm to ensure irradiation with visible light only. For MB photodegradation experiments: 0.2 g of the as-prepared CeO_2–$BiVO_4$/FAC catalyst was dispersed in MB solution (50 mL, 10 mg/L) by ultrasonic treatment. Prior to irradiation, the suspensions were magnetically stirred in the dark for 30 min to obtain MB adsorption–desorption equilibrium. At given time intervals, 4 mL of the suspension was collected, the catalyst was separated by filtration and the concentration (C) of the remaining MB solution was determined from UV–vis absorption measurements by using the Beer–Lambert law relation at the maximum absorption wavelength (λ_{max}) of 664 nm. For comparison, the photocatalytic degradation of MB by the pure $BiVO_4$ and pure CeO_2 was performed using the same procedure as above.

2. Results and discussion

2.1. X-ray diffraction

Fig. 1 presents the XRD diffraction patterns of the pristine (uncoated) FACs, pure CeO_2 and CeO_2–$BiVO_4$/FAC composites. In Fig. 1 line c and line d, the characteristic peaks at 18.5, 35

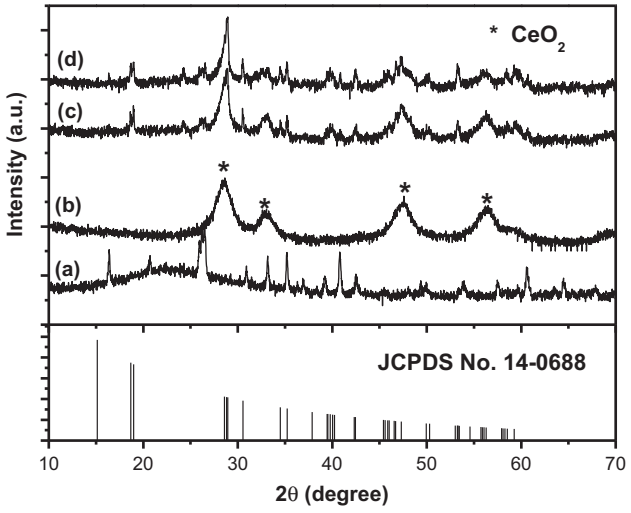

Fig. 1 – XRD diffraction patterns. (a) pristine FACs; (b) pure CeO_2; (c) 10 wt.% CeO_2–$BiVO_4$/FACs; (d) 7.5 wt.% CeO_2–$BiVO_4$/FACs.

and 46° are split, and peaks also observed at 28.6, 30.5, 39.7 and 53.1° are indexed to the monoclinic scheelite structure of $BiVO_4$ (JCPDS No. 14-0688). Diffraction peaks of pure CeO_2 at 2θ of 28.8, 33.3, 47.6, and 56.4° can be indexed as the (111), (200), (220), and (311) planes of the face-centered cubic structure of CeO_2 (JCPDS No. 34-0394) (Wetchakun et al., 2012). The XRD patterns of CeO_2–$BiVO_4$/FAC composites exhibited characteristic diffraction peaks of both $BiVO_4$ and CeO_2 crystalline phases.

2.2. SEM/EDX analysis

SEM micrographs of the FAC and CeO_2–$BiVO_4$/FAC composites are shown in Fig. 2. It can be seen clearly from Fig. 2a and b that the pristine FACs have a regular spherical surface morphology with diameter of 100–120 μm, and the cenosphere surface is smooth. The chemical composition of the cenospheres was revealed by EDX analysis (Fig. 2e) and shows that they are composed mainly of Si, Al, C, and O elements, with small amounts of elements such as Mg, Fe, Ti and K also observed. Compared with the smooth surface of the pristine cenospheres, Fig. 2c and d shows that the surface of the FACs is covered with a layer of CeO_2–$BiVO_4$ composite particles. The size of particles roughly estimated is about 200–300 nm. The corresponding EDX spectrum (Fig. 2f) exhibits the characteristic peaks of elemental Bi, V and Ce in the composites. The combined results of SEM and EDX suggest that the CeO_2–$BiVO_4$ junction composites were coated successfully on the surface of FACs by this MOD and impregnation method.

2.3. XPS analysis

To evaluate the electronic state of the as-prepared CeO_2–$BiVO_4$/FAC composites, XPS techniques were employed in this study. Fig. 3 shows the XPS spectra of the pristine FACs, $BiVO_4$ film coated FACs ($BiVO_4$/FACs), and the CeO_2–$BiVO_4$/FAC composites. The surface of the pristine FACs is composed mainly of Si, Al, O and C, while new Bi 4f, V 2p, and Ce 3d peaks at bonding energies (BE) of around 160, 520, and 900 eV, respectively, became clearly visible in the XPS spectra of the CeO_2–$BiVO_4$/FAC composite.

Fig. 4a and d shows Bi4f, V2p, Ce3d and O1s high-resolution XPS spectra of the as-fabricated CeO_2–$BiVO_4$/FAC composites. In Fig. 4a, the sample exhibits spin-orbit splitting signals of Bi $4f_{7/2}$ and Bi $4f_{5/2}$ at BE = 158 and 163 eV, which were characteristic of Bi^{3+}. The XPS spectra of V2p (Fig. 4b) show that two peaks were present; the first peak situated around 516 eV is ascribed to V $2p_{3/2}$; the other peak at approximately 523 eV is ascribed to V $2p_{1/2}$. Fig. 4c presents the XPS spectra for the Ce 3d region of the CeO_2–$BiVO_4$/FAC composites. In Fig. 4c, peaks labeled

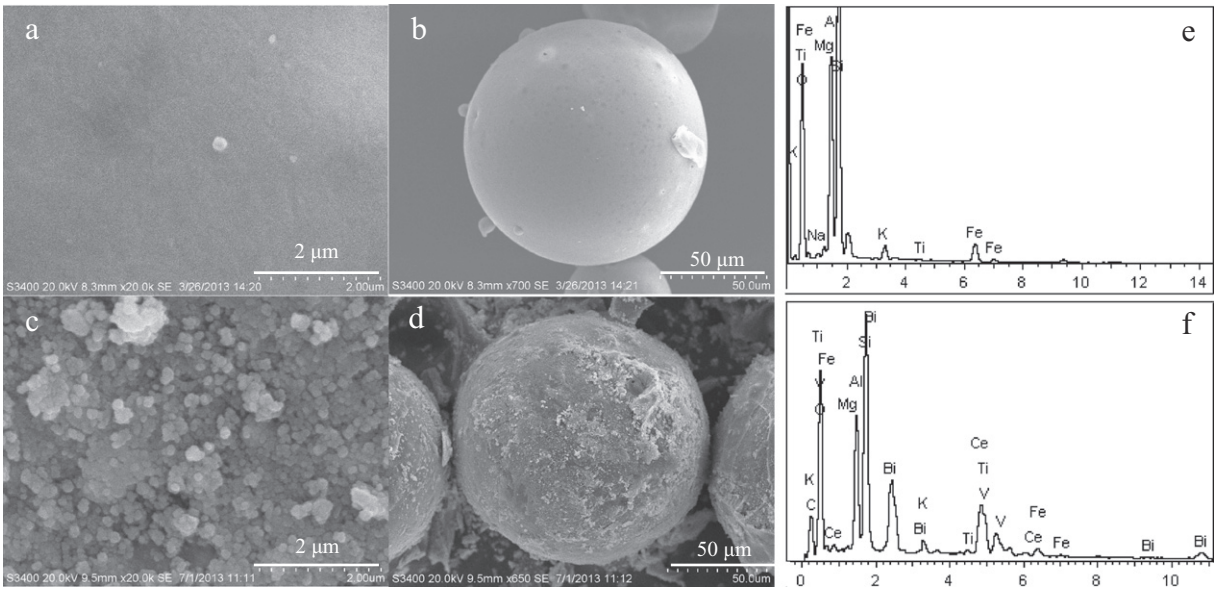

Fig. 2 – SEM micrographs of a pristine FAC at low (a) and high magnification (b), CeO_2–$BiVO_4$/FACs at low (c) and high (d) magnification; EDX spectra of pristine FAC (e) and CeO_2–$BiVO_4$/FAC samples (f).

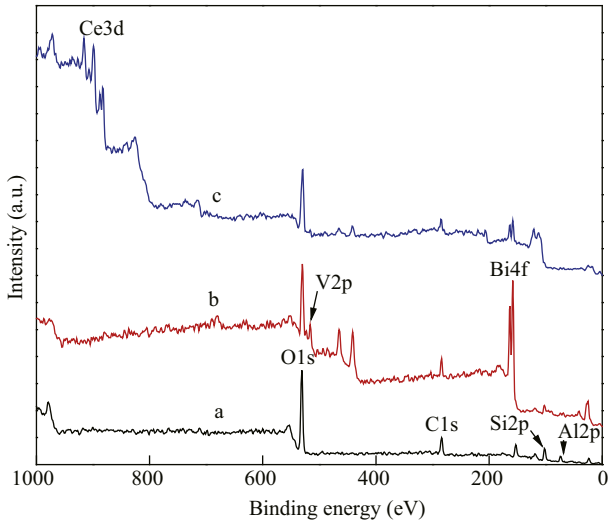

Fig. 3 – XPS spectra of pristine FACs (a); $BiVO_4$/FACs (b), and CeO_2–$BiVO_4$/FAC samples (c).

as *v* arise from $3d_{5/2}$ photoemissions, whereas associated $3d_{3/2}$ emissions are labeled as *u*. Spin–orbit peaks of *v‴* and *u‴* at 897.5 and 916.0 eV with 18.5 eV separation are attributed to primary photoionization from Ce^{4+} with $Ce3d^94f^0O2p^6$ final state. Lower binding energy states of *v″* (886.6 eV)–*u″* (906.7 eV) and *v* (881.8 eV)–*u* (899.8 eV) have been assigned to the $Ce3d^94f^1O2p^5$ and $Ce3d^94f^2O2p^4$ final state shake-down satellite features (Fernandes et al., 2012; Mullins et al., 1998; Zhou et al., 2010). Satellites are caused by the facilitation of ligand (O2p) to metal (Ce4f) charge transfer by the primary photoionization process. Peaks labeled as *v′* and *u′* at 884.3 and 902.8 eV are associated with Ce^{3+} final states, which are assigned to the main photoionization from the $Ce3d^94f^1O2p^6$ final state (Fernandes et al., 2012; Mullins et al., 1998; Anandan et al., 2013). XPS data are useful in interpretation of the results of XRD analysis, displaying the film diffraction peaks that correspond only to CeO_2. Taking into account XPS findings, this can be explained by the completely oxidized (CeO_2) top surface layer as well as by the mixed CeO_2 + Ce_2O_3 oxide region under it (Ershov et al., 2013; Paparazzo et al., 1991). In Fig. 4d, O1s spectra were fitted with two peaks; the components at BE = 528.6 eV are characteristic of the lattice oxide (OI) species, while the components at BE = 531.1 eV belong to the adsorbed oxygen (OII) species (Yang et al., 2005).

2.4. DRS analysis

The UV–vis diffuse reflection spectra of pure $BiVO_4$, pure CeO_2 and CeO_2–$BiVO_4$/FAC composite are depicted in Fig. 5. The absorption edge of the CeO_2–$BiVO_4$/FAC composites shows a shift toward the visible region, and the CeO_2–$BiVO_4$/FAC composites exhibit enhanced absorption compared to that of with pure $BiVO_4$ and pure CeO_2 within the region 525–800 nm. The band gap absorption edges of pure CeO_2, pure $BiVO_4$, and 7.5 wt.% CeO_2–$BiVO_4$/FAC composite are at about 449, 527, and 601 nm,

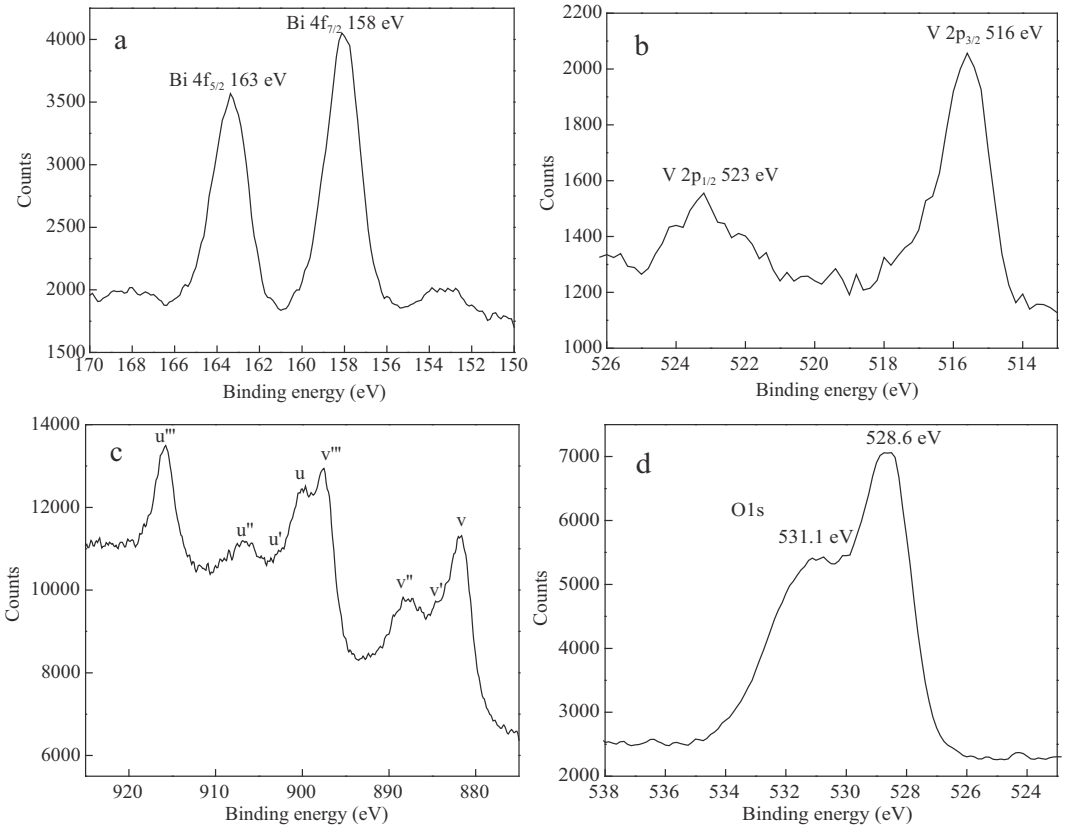

Fig. 4 – High resolution XPS spectrum analysis of Bi 4f (a); V 2p (b); Ce 3d (c) and O 1s (d) on the surface of the CeO_2–$BiVO_4$/FAC sample.

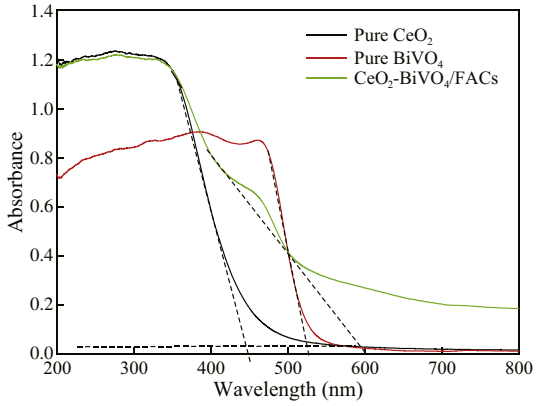

Fig. 5 – UV–Vis diffuse reflectance spectra of different samples.

and their band gap energies (E_g) are calculated to be 2.78, 2.37 and 2.08 eV, respectively. These results indicate that the CeO_2–$BiVO_4$/FAC composites can be photoexcited to generate more electron–hole pairs under visible-light irradiation, which would result in higher photocatalytic degradation efficiency (Wetchakun et al., 2012).

2.5. *Photocatalytic activity testing*

The photocatalytic activity of the samples was evaluated by the degradation of MB aqueous solution. Fig. 6 displays the degradation of MB solution in the presence of different samples. As seen in Fig. 6a, a blank test without the photocatalyst under visible light irradiation shows that the photolysis of MB was negligible. As a comparison, the photodegradation of MB with pure $BiVO_4$, pure CeO_2, $BiVO_4$/FACs and CeO_2/FACs was also performed. About 22%, 40%, 43% and 70% of MB were removed over the pure CeO_2, CeO_2/FACs, pure $BiVO_4$ and $BiVO_4$/FAC catalysts within 180 min, respectively. It was obvious that a synergistic effect occurred between $BiVO_4$ and the FACs, leading to the enhancement of photocatalytic activity.

Moreover, it was found that the CeO_2–$BiVO_4$/FAC composites showed better photocatalytic activities than the pure $BiVO_4$, indicating that the CeO_2 loading on $BiVO_4$ played a role in the enhancement of photocatalytic activity. The optimal content of CeO_2 on $BiVO_4$/FACs was about 7.5 wt.% from our experimental results; and less photocatalytic activity was observed with higher CeO_2 content. The best photodegradation rate was as high as 90% over the 7.5 wt.% CeO_2–$BiVO_4$/FAC photocatalyst in 180 min. Further increasing the cerium content up to 10 wt.% led to a decline in the catalytic activity. There are two factors that limited performance at high Ce loading: (1) blockage of active sites by excess amounts of Ce introduced in the photocatalysts and (2) an increase in opacity and light scattering of CeO_2–$BiVO_2$ nanoparticles at a high concentration leads to a decrease in the passage of light through the sample (Ghasemi et al., 2012; Yang et al., 2007).

It has been demonstrated that the photocatalytic degradation of MB follows Langmuir–Hinshelwood first-order reaction kinetics behavior (Hiroaki et al., 1998; Fu et al., 2011). The rate constant (k) can be calculated for the photocatalytic degradation of MB under visible-light irradiation at 25°C according to Eq. (1).

$$k = \frac{1}{t} 1n \frac{C_0}{C_t} \quad (1)$$

where, k (min^{-1}) is the first-order rate constant, and C_0 and C_t are the concentration of MB when reaction time is 0 and t (min), respectively.

The first-order kinetics dependence of the photocatalytic degradation ratio for the different samples is shown in Fig. 6b. In Table 1, the values of rate constant (k) are 0.00155, 0.00284, 0.00295, 0.00601, and 0.01307 min^{-1} corresponding to the pure CeO_2, CeO_2/FACs, pure $BiVO_4$, $BiVO_4$/FACs and 7.5 wt.% CeO_2–$BiVO_4$/FACs, respectively. Clearly, the k value of 7.5 wt.% CeO_2–$BiVO_4$/FACs was 4.4 and 2.1 times greater than that of pure $BiVO_4$ and $BiVO_4$/FAC samples, respectively.

The enhanced photocatalytic activity over the CeO_2–$BiVO_4$/FAC composite photocatalyst may be attributable to the following: (1) Cerium oxide has a multi-functional role. It traps electrons, which retards electron–hole recombination and increases the amount of $.O_2^-$ for degradation of the pollutants by Reactions (2)–(6) (Ghasemi et al., 2012); and (2) the p–n-type

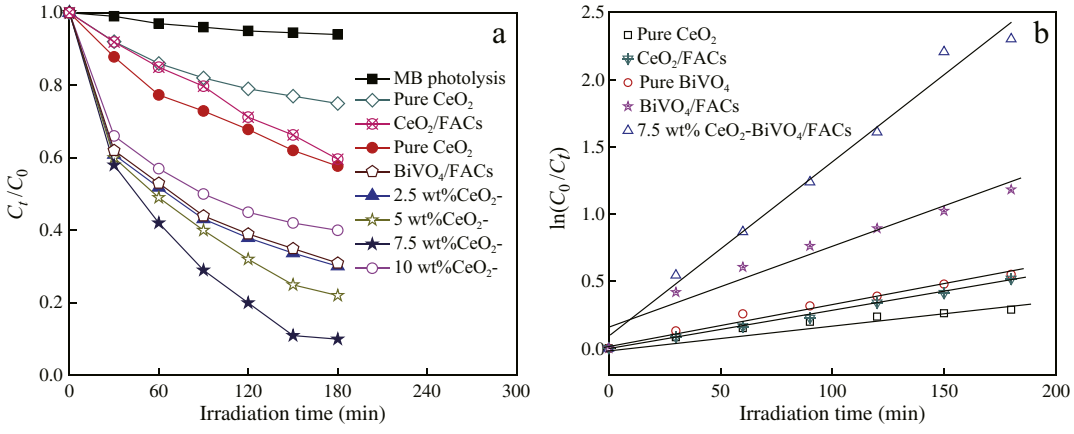

Fig. 6 – Photocatalytic activity of different samples (a) and variations in $ln(C_0 / C_t)$ as a function of irradiation time (b).

Table 1 – Rate constants of MB photodecomposition and linear regression coefficients from a plot of $\ln(C_0 / C_t) = kt$ with different samples.

Photocatalysts	Regression equation	R^2	k (min^{-1})
Pure CeO_2	$y = 0.00155x + 0.03404$	0.9743	0.00155
CeO_2/FACs	$y = 0.00284x - 0.00671$	0.9951	0.00284
Pure $BiVO_4$	$y = 0.00295x + 0.03709$	0.9916	0.00295
$BiVO_4$/FACs	$y = 0.00601x + 0.1570$	0.9547	0.00601
7.5 wt.% CeO_2–$BiVO_4$/FACs	$y = 0.01303x + 0.07682$	0.9831	0.01303

heterojunction formed between CeO_2 and $BiVO_4$. The holes (h^+) on the valence band of n-type $BiVO_4$ transfer to that of p-type CeO_2, while the photogenerated electrons (e^-) in the conduction band of n-type $BiVO_4$ cannot transfer to that of p-type CeO_2, improving the separation of photoinduced electron–hole pairs in $BiVO_4$, resulting in higher photocatalytic activity (Wetchakun et al., 2012; Jang et al., 2012); (3) the introduction of FACs helps avoid aggregation of particles, which contributes to making full use of light for photocatalysis (Phanikrishna et al., 2008); and (4) the concerted effects of $BiVO_4$ and FACs or their integrated properties (Fu et al., 2011).

$$BiVO_4 + h\nu \rightarrow e_{CB}^- + h_{VB}^+ \quad (2)$$

$$Ce^{4+} + e_{CB}^- \rightarrow Ce^{3+} \quad (3)$$

$$Ce^{3+} + O_2 \rightarrow Ce^{4+} + \cdot O_2^- \quad (4)$$

$$\cdot O_2^- + 2H_2O \rightarrow \cdot OH + OH^- \quad (5)$$

$$MB + \cdot OH \rightarrow \text{degradation products.} \quad (6)$$

It is well known that the stability of a practical photocatalyst is very important as well as its photocatalytic activity. The as-prepared 7.5 wt.% CeO_2–$BiVO_4$/FAC photocatalyst was further investigated in recycling experiments. After the 1st cycle, the catalyst was removed from aqueous solution, and then it was washed with water and dried at 110°C for 2 hr. Fig. 7 shows results from five successive runs for the photodegradation of MB under the same experimental conditions. However, after 5 runs a slight decrease of photocatalytic efficiency for degradation of MB dyes could be observed. This effect is attributed to two main reasons: one is the loss of some $BiVO_4$ from the surface; the other is fouling of the catalyst by the by-products of degradation. Such fouling of the catalyst surface also occurs for suspended $BiVO_4$, and can be partly cleaned by exposing the catalyst for a long time of irradiation (Rao et al., 2004).

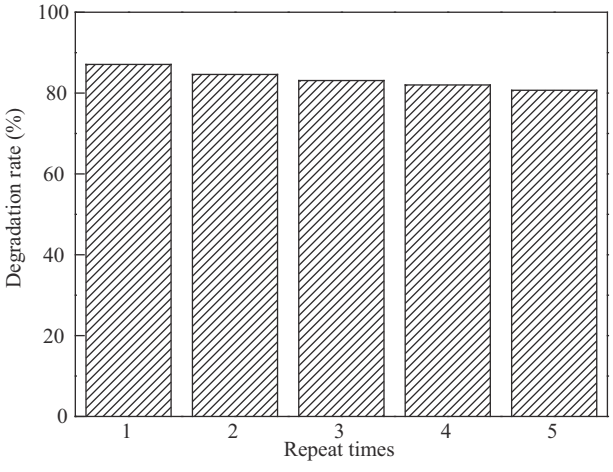

Fig. 7 – Recycling test of 7.5 wt.% CeO_2–$BiVO_4$/FACs under visible light irradiation (photocatalyst of 4 g/L; MB of 10 mg/L and irradiation time of 180 min).

3. Conclusions

Novel CeO_2–$BiVO_4$/FAC composite photocatalysts were successfully prepared by MOD and impregnation methods. Ce loading enhanced the visible-light absorption of the catalysts, and the Ce-loaded samples exhibited higher photocatalytic activity in comparison with pure $BiVO_4$ and pure CeO_2. The 7.5 wt.% CeO_2–$BiVO_4$/FAC composite showed the highest photocatalytic activity for MB degradation under visible light irradiation. The composites can be easily separated from water after the reaction due to their low density. The recycling test revealed that the composites were quite stable after repeated use for more than 5 times. Thus, the CeO_2–$BiVO_4$/FAC catalyst is a promising candidate for the photodegradation of dyes from wastewater.

Acknowledgments

The authors gratefully acknowledge financial support from the Natural Science Foundation of China (No. 51008154), the China Postdoctoral Science Foundation funded project (No. 2012M511254) and the Natural Science Research Project of Jiangsu Province's Education Department (No. 12KJD610004).

REFERENCES

Anandan, C., Bera, P., 2013. XPS studies on the interaction of CeO_2 with silicon in magnetron sputtered CeO_2 thin films on Si and Si_3N_4 substrates. Appl. Surf. Sci. 283, 297–303.

Ershov, S., Druart, M.E., Poelman, M., Cossement, D., Snyders, R., Olivier, M.G., 2013. Deposition of cerium oxide thin films by reactive magnetron sputtering for the development of corrosion protective coatings. Corros. Sci. 75, 158–168.

Fernandes, V., Graff, I.L., Varald, J., Amaral, L., Fichtner, P., Demaille, D., et al., 2012. Valence evaluation of cerium in

nanocrystalline CeO_2 films electrodeposited on Si substrates. J. Electrochem. Soc. 159 (1), K27–K36.
Foletto, E.L., Battiston, S., Collazzo, G.C., Bassaco, M.M., Mazutti, M.A., 2012. Degradation of leather dye using CeO_2–SnO_2 nanocomposite as photocatalyst under sunlight. Water Air Soil Pollut. 223 (9), 5773–5779.
Fu, Y.S., Sun, X.Q., Wang, X., 2011. $BiVO_4$–graphene catalyst and its high photocatalytic performance under visible light irradiation. Mater. Chem. Phys. 131 (1–2), 325–330.
Galembeck, A., Alves, O.L., 2002. Bismuth vanadate synthesis by metallo-organic decomposition: thermal decomposition study and particle size control. J. Mater. Sci. 37 (10), 1923–1927.
Ghasemi, S., Setayesh, S., Habibi-Yangjeh, R., Hormozi-Nezhad, A., Gholami, M.R., 2012. Assembly of CeO_2–TiO_2 nanoparticles prepared in room temperature ionic liquid on graphene nanosheets for photocatalytic degradation of pollutants. J. Hazard. Mater. 199–200, 170–178.
Hernández-Alonso, M.D., Hungría, A.B., Martínez-Arias, A., Fernández-García, M., Coronado, J.M., Conesa, J.C., et al., 2004. EPR study of the photoassisted formation of radicals on CeO_2 nanoparticles employed for toluene photooxidation. Appl. Catal. B 50 (3), 167–175.
Hiroaki, T., Manabu, A., Yasuyuki, K., Seishiro, I., 1998. Enhancing effect of SiO_x monolayer coverage of TiO_2 on the photoinduced oxidation of rhodamine 6G in aqueous media. J. Phys. Chem. B 102 (33), 6360–6366.
Jang, J.S., Kim, H.G., Lee, S.H., 2012. Efficient photocatalytic degradation of Acid Orange 7 on metal oxide p–n junction composites under visible light. J. Phys. Chem. Solid 73 (11), 1372–1377.
Jeong, H.W., Jeon, T.H., Jang, J.S., Choi, W.Y., 2013. Strategic modification of $BiVO_4$ for improving photoelectrochemical water oxidation performance. J. Phys. Chem. C 117 (18), 9104-9012.
Kubacka, A., Fernández-García, M., Colón, G., 2012. Advanced nanoarchitectures for solar photocatalytic applications. Chem. Rev. 112 (3), 1555–1614.
Ma, B.W., Guo, J.F., Dai, W.L., Fan, K.N., 2012. Ag–AgCl/WO_3 hollow sphere with flower-like structure and superior visible photocatalytic activity. Appl. Catal. B. 123–124, 193–199.
Mullins, D.R., Overbury, S.H., Huntley, D.R., 1998. Electron spectroscopy of single crystal and polycrystalline cerium oxide surfaces. Surf. Sci. 409 (2), 307–319.
Muńnoz-Batista, M.J., Kuback, A., Gómez-Cerezo, M.N., Tudela, D., Fernández-García, M., 2013. Sunlight-driven toluene photo-elimination using CeO_2–TiO_2 composite systems: a kinetic study. Appl. Catal. B 140–141, 626–635.
Naya, S.I., Tanaka, M., Kimura, K., Tada, H., 2011. Visible-light-driven copper acetylacetonate decomposition by $BiVO_4$. Langmuir 27 (16), 10334–10339.
Obregón, S., Caballero, A., Colón, G., 2012. Hydrothermal synthesis of $BiVO_4$: structural and morphological influence on the photocatalytic activity. Appl. Catal. B 117–118, 59–66.
Pang, J.F., Li, Q., Wang, B., Tao, D.J., Xu, X.T., Wang, W., et al., 2012. Preparation and characterization of electroless Ni–Fe–P alloy films on fly ash cenospheres. Powder Technol. 226, 246–252.
Paparazzo, E., Ingo, G.M., Zacchetti, N., 1991. X-ray induced reduction effects at CeO_2 surfaces—an X-ray Photoelectron-Spectroscopy study. J. Vacuum Sci. Technol. 9 (3), 1416–1420.
Park, H.S., Kweon, K.E., Ye, H.C., Paek, E., Hwang, G.S., Bard, A.J., 2011. Factors in the metal doping of $BiVO_4$ for improved photoelectrocatalytic activity as studied by scanning electrochemical microscopy and first-principles density-functional calculation. J. Phys. Chem. C 115 (36), 17870–17879.
Phanikrishna Sharma, M.V., Kumari, V.D., Subrahmanyam, A., 2008. Photocatalytic degradation of isoproturon herbicide over TiO_2/Al-MCM-41 composite systems using solar light. Chemosphere 72, 644–651.
Rao, K.V.S., Subrahmanyam, M., Boule, P., 2004. Immobilized TiO_2 photocatalyst during long-term use: decrease of its activity. Appl. Catal. B 49 (4), 239–249.
Ren, L., Ma, L., Jin, L., Wang, J.B., Qiu, M., Yu, Y., 2009. Template-free synthesis of $BiVO_4$ nanostructures: II. Relationship between various microstructures for monoclinic $BiVO_4$ and their photocatalytic activity for the degradation of rhodamine B under visible light. Nanotechnology 20 (40), 405602. http://dx.doi.org/10.1088/0957-4484/20/40/405602.
Shao, Y., Ma, Y., 2012. Mesoporous CeO_2 nanowires as recycled photocatalysts. Sci. China Chem. 55 (7), 1303–1307.
Wang, W.J., Yu, Y., An, T.C., Li, G.Y., Yip, H.Y., Yu, J.C., et al., 2012. Visible-light-driven photocatalytic inactivation of *E. coli* K-12 by bismuth vanadate nanotubes: bactericidal performance and mechanism. Environ. Sci. Technol. 46 (8), 4599–4606.
Wetchakun, N., Chaiwichain, S., Inceesungvorn, B., Pingmuang, K., Phanichphant, S., Minett, A.I., et al., 2012. $BiVO_4$/CeO_2 nanocomposites with high visible-light-induced photocatalytic activity. ACS Appl. Mater. Interfaces 4 (7), 3718–3723.
Won, J.J., Jang, J.W., Kong, K.J., Kang, H.J., Kim, J.Y., Jun, H., et al., 2012. Phosphate doping into monoclinic $BiVO_4$ for enhanced photoelectrochemical water oxidation activity. Angew. Chem. Int. Ed. 51 (24), 3147–3151.
Yang, S.X., Feng, Y., Wan, J., Zhu, W., Jiang, Z., 2005. Effect of CeO_2 addition on the structure and activity of RuO_2/c-Al_2O_3 catalyst. Appl. Surf. Sci. 246 (1–3), 222–228.
Yang, H., Zhang, K., Shi, R., 2007. Sol–gel synthesis and photocatalytic activity of CeO_2/TiO_2 nanocomposites. J. Am. Ceram. Soc. 90 (5), 1370–1374.
Zhang, L.L., Lv, F.J., Zhang, W.G., Li, R.Q., Zhong, H., Zhao, Y.J., et al., 2009. Photo degradation of methyl orange by attapulgite–SnO_2–TiO_2 nanocomposites. J. Hazard. Mater. 171 (1–3), 294–300.
Zhang, J., Cui, H., Wang, B., Li, C., Zhai, J.P., Li, Q., 2013. Fly ash cenospheres supported visible-light-driven $BiVO_4$ photocatalyst: synthesis, characterization and photocatalytic application. Chem. Eng. J. 223, 737–746.
Zhao, W.R., Wang, Y., Yang, Y., Tang, J., Yang, Y., 2012. Carbon spheres supported visible-light-driven CuO–$BiVO_4$ heterojunction: preparation, characterization, and photocatalytic properties. Appl. Catal. B 115–116, 90–99.
Zhao, Z.X., Dai, H.X., Deng, J.G., Liu, Y.X., Wang, Y., Li, X.W., et al., 2013. Porous FeOx/$BiVO_4$–δS0.08: highly efficient photocatalysts for the degradation of Methylene Blue under visible-light illumination. J. Environ. Sci. 25 (10), 2138–2149.
Zhou, Y.H., Perket, J.M., Zhou, J., 2010. Growth of Pt nanoparticles on reducible CeO_2 (111) thin films: effect of nanostructures and redox properties of Ceria. J. Phys. Chem. C 114, 11853–11860.
Zhou, Z.J., Long, M.C., Cai, W.M., Cai, J., 2012. Synthesis and photocatalytic performance of the efficient visible light photocatalyst Ag–AgCl/$BiVO_4$. J. Mol. Catal. A 353–354, 22–28.

Editorial Board of Journal of Environmental Sciences

Editor-in-Chief

Hongxiao Tang Research Center for Eco-Environmental Sciences, Chinese Academy of Sciences, China

Associate Editors-in-Chief

Jiuhui Qu Research Center for Eco-Environmental Sciences, Chinese Academy of Sciences, China
Shu Tao Peking University, China
Nigel Bell Imperial College London, United Kingdom
Po-Keung Wong The Chinese University of Hong Kong, Hong Kong, China

Editorial Board

Aquatic environment

Baoyu Gao
Shandong University, China
Maohong Fan
University of Wyoming, USA
Chihpin Huang
National Chiao Tung University
Taiwan, China
Ng Wun Jern
Nanyang Environment &
Water Research Institute, Singapore
Clark C. K. Liu
University of Hawaii at Manoa, USA
Hokyong Shon
University of Technology, Sydney, Australia
Zijian Wang
Research Center for Eco-Environmental Sciences,
Chinese Academy of Sciences, China
Zhiwu Wang
The Ohio State University, USA
Yuxiang Wang
Queen's University, Canada
Min Yang
Research Center for Eco-Environmental Sciences,
Chinese Academy of Sciences, China
Zhifeng Yang
Beijing Normal University, China
Han-Qing Yu
University of Science & Technology of China

Terrestrial environment

Christopher Anderson
Massey University, New Zealand
Zucong Cai
Nanjing Normal University, China
Xinbin Feng
Institute of Geochemistry,
Chinese Academy of Sciences, China
Hongqing Hu
Huazhong Agricultural University, China
Kin-Che Lam
The Chinese University of Hong Kong
Hong Kong, China
Erwin Klumpp
Research Centre Juelich, Agrosphere Institute
Germany
Peijun Li
Institute of Applied Ecology,
Chinese Academy of Sciences, China
Michael Schloter
German Research Center for Environmental Health
Germany
Xuejun Wang
Peking University, China
Lizhong Zhu
Zhejiang University, China

Atomospheric environment

Jianmin Chen
Fudan University, China
Abdelwahid Mellouki
Centre National de la Recherche Scientifique
France
Yujing Mu
Research Center for Eco-Environmental Sciences,
Chinese Academy of Sciences, China
Min Shao
Peking University, China
James Jay Schauer
University of Wisconsin-Madison, USA
Yuesi Wang
Institute of Atmospheric Physics,
Chinese Academy of Sciences, China
Xin Yang
University of Cambridge, UK

Environmental biology

Yong Cai
Florida International University, USA
Henner Hollert
RWTH Aachen University, Germany
Jae-Seong Lee
Sungkyunkwan University, South Korea
Christopher Rensing
University of Copenhagen, Denmark
Bojan Sedmak
National Institute of Biology, Slovenia
Lirong Song
Institute of Hydrobiology,
Chinese Academy of Sciences, China
Chunxia Wang
National Natural Science Foundation of China
Gehong Wei
Northwest A & F University, China
Daqiang Yin
Tongji University, China
Zhongtang Yu
The Ohio State University, USA

Environmental toxicology and health

Jingwen Chen
Dalian University of Technology, China
Jianying Hu
Peking University, China
Guibin Jiang
Research Center for Eco-Environmental Sciences,
Chinese Academy of Sciences, China
Sijin Liu
Research Center for Eco-Environmental Sciences,
Chinese Academy of Sciences, China
Tsuyoshi Nakanishi
Gifu Pharmaceutical University, Japan
Willie Peijnenburg
University of Leiden, The Netherlands
Bingsheng Zhou
Institute of Hydrobiology,
Chinese Academy of Sciences, China

Environmental catalysis and materials

Hong He
Research Center for Eco-Environmental Sciences,
Chinese Academy of Sciences, China
Junhua Li
Tsinghua University, China
Wenfeng Shangguan
Shanghai Jiao Tong University, China
Yasutake Teraoka
Kyushu University, Japan
Ralph T. Yang
University of Michigan, USA

Environmental analysis and method

Zongwei Cai
Hong Kong Baptist University,
Hong Kong, China
Jiping Chen
Dalian Institute of Chemical Physics,
Chinese Academy of Sciences, China
Minghui Zheng
Research Center for Eco-Environmental Sciences,
Chinese Academy of Sciences, China

Municipal solid waste and green chemistry

Pinjing He
Tongji University, China

Environmental ecology

Rusong Wang
Research Center for Eco-Environmental Sciences,
Chinese Academy of Sciences, China

Editorial office staff

Managing editor Qingcai Feng
Editors Zixuan Wang Suqin Liu Zhengang Mao
English editor Catherine Rice (USA)

Copyright© Research Center for Eco-Environmental Sciences, Chinese Academy of Sciences. Published by Elsevier B.V. and Science Press. All rights reserved.

JOURNAL OF ENVIRONMENTAL SCIENCES

环境科学学报(英文版)

(http://www.jesc.ac.cn)

Aims and scope

Journal of Environmental Sciences is an international academic journal supervised by Research Center for Eco-Environmental Sciences, Chinese Academy of Sciences. The journal publishes original, peer-reviewed innovative research and valuable findings in environmental sciences. The types of articles published are research article, critical review, rapid communications, and special issues.

The scope of the journal embraces the treatment processes for natural groundwater, municipal, agricultural and industrial water and wastewaters; physical and chemical methods for limitation of pollutants emission into the atmospheric environment; chemical and biological and phytoremediation of contaminated soil; fate and transport of pollutants in environments; toxicological effects of terrorist chemical release on the natural environment and human health; development of environmental catalysts and materials.

For subscription to electronic edition

Elsevier is responsible for subscription of the journal. Please subscribe to the journal via http://www.elsevier.com/locate/jes.

For subscription to print edition

China: Please contact the customer service, Science Press, 16 Donghuangchenggen North Street, Beijing 100717, China. Tel: +86-10-64017032; E-mail: journal@mail.sciencep.com, or the local post office throughout China (domestic postcode: 2-580).

Outside China: Please order the journal from the Elsevier Customer Service Department at the Regional Sales Office nearest you.

Submission declaration

Submission of an article implies that the work described has not been published previously (except in the form of an abstract or as part of a published lecture or academic thesis), that it is not under consideration for publication elsewhere. The submission should be approved by all authors and tacitly or explicitly by the responsible authorities where the work was carried out. If the manuscript accepted, it will not be published elsewhere in the same form, in English or in any other language, including electronically without the written consent of the copyright-holder.

Submission declaration

Submission of the work described has not been published previously (except in the form of an abstract or as part of a published lecture or academic thesis), that it is not under consideration for publication elsewhere. The publication should be approved by all authors and tacitly or explicitly by the responsible authorities where the work was carried out. If the manuscript accepted, it will not be published elsewhere in the same form, in English or in any other language, including electronically without the written consent of the copyright-holder.

Editorial

Authors should submit manuscript online at http://www.jesc.ac.cn. In case of queries, please contact editorial office, Tel: +86-10-62920553, E-mail: jesc@263.net, jesc@rcees.ac.cn. Instruction to authors is available at http://www.jesc.ac.cn.

Journal of Environmental Sciences (Established in 1989)

Vol. 26 No. 9 2014

Supervised by	Chinese Academy of Sciences	**Published by**	Science Press, Beijing, China
Sponsored by	Research Center for Eco-Environmental		Elsevier Limited, The Netherlands
	Sciences, Chinese Academy of Sciences	**Distributed by**	
Edited by	Editorial Office of Journal of	Domestic	Science Press, 16 Donghuangchenggen
	Environmental Sciences		North Street, Beijing 100717, China
	P. O. Box 2871, Beijing 100085, China		Local Post Offices through China
	Tel: 86-10-62920553; http://www.jesc.ac.cn	Foreign	Elsevier Limited
	E-mail: jesc@263.net, jesc@rcees.ac.cn		http://www.elsevier.com/locate/jes
Editor-in-chief	Hongxiao Tang	**Printed by**	Beijing Beilin Printing House, 100083, China

CN 11-2629/X **Domestic postcode: 2-580** **Domestic price per issue RMB ¥ 110.00**

ISSN 1001-0742

09>

9 771001 074147